

Distribution of Radioelements and its Relation to Uranium Migration, El-Erediya Exploratory Tunnels, Central Eastern Desert, Egypt

ALI ABU-DEIF

HELMY S.O. ABOUENAGA and HAMDY I.E. HASSANEIN
Nuclear Materials Authority, El Maadi, Cairo, Egypt

Received: 11/9/2001 Revised: 9/3/2002 Accepted: 12/10/2002

ABSTRACT. Uranium mineralization, connected mainly to jasperoid veins, occupying shear and fracture zones, was discovered in 1970 at El-Erediya post-tectonic granitic mass, Central Eastern Desert, Egypt. Exploratory tunnels were excavated, at wadi (valley) level, following these shear zones, in order to determine extensions of the mineralized parts and evaluate their potentiality. Excavation works revealed the presence of massive and disseminated pitchblende, as well as its secondary associations, in some sections of the explored shear zones. The granite along the shear zone is more or less altered. The main alteration features are silicification, mylonitization, kaolinization and, to a less extent, sericitization. An extensive gamma-ray spectrometric survey was carried out on two of the mineralized sections and the unaltered granite. Spectrometric data were statistically treated in order to evaluate the uranium potentiality and its migration trend. The study shows that there is a close relationship between the distribution of radioelements and the lithology. It also shows that migration of uranium took place inside in the silicified granite, while the migration is in outward in case of the pink and kaolinized granite.

Introduction

The Gamma-ray spectrometric method is a powerful tool in geological mapping; it is possible to determine the individual concentrations of the three naturally occurring radioelements in the ground. The method depends upon the fact that the absolute and relative concentrations of the radioelements, K, U, and Th

vary measurably and significantly with lithology (Darnley and Ford, 1989). The distribution of these radioelements at the surface is controlled by bedrock composition and modified by a variety of geologic processes, the most dominant being weathering, erosion, and transportation (Pitkin and Duval, 1980). Ong and Mior Shallehuddin (1988), in their analysis of promising uranium prospects in the central belt area of Peninsular Malaysia, concluded that using maps of eTh, eU and K permits better analysis of petrographic differentiation according to the spectral response, and the parameters of eU/eTh, eU/K and eTh/K reflect the radioactive character of the rock. They reported that: if $eTh/K \geq 2 \times 10^{-4}$, the rock is thorium rich, if $eTh/K \leq 1 \times 10^{-4}$, the rock is potassium rich and if $eU/eTh \geq 1$ and $eU/K \geq 1 \times 10^{-4}$, the rock is uranium rich. The main topic of this work is to study the distribution of the radioelements in El-Erediya tunnels in order to clarify their relation to the different alterations and to detect some radiometric parameters related to the uranium mineralization and its migration.

Geologic Setting

El-Erediya post-tectonic granitic mass is located some 25 km to the south of km 85, Qena-Safaga highway, Fig. 1. It is emplaced, within the Precambrian basement rocks south of the major lithotectonic discontinuity that forms the border contact between the Central and the North Eastern Desert tectonic blocks (Stern and Hedge, 1985). It forms a thick sheet (6.5×2.5 km), trending in NW direction parallel to the Red Sea, intruded mainly into metamorphosed basic rocks comprising parts of the ophiolitic-island arc sequence. In some parts, the surrounding country rocks have undergone thermal metamorphism along their contact with the granite. Dykes and veins of aplites, porphyries, pegmatite and jasper as well as few basaltic dikes dissect the granite. It has been emplaced during the post-tectonic episode in Egypt, about 600 Ma (Greenberg, 1981). Rb-Sr age reported for El-Erediya is 570 ± 5 Ma (Fullagar, 1980), whereas U-Pb age reported by Abu-Deif (1992) is 583 ± 21 Ma. The granitic mass of El Erediya is an epizonal-undeformed leucocratic mass displaying a good degree of uniformity in both texture and mineralogy. The granite is greyish pink to red in colour, medium-to coarse-grained. It is essentially composed of alkali feldspars (microcline and orthoclase), some of that occur as large elongated crystals, sodic plagioclase, and quartz (sometimes smoky in colour) and subordinate amounts of biotite. Accessory minerals are sphene, apatite, magnetite and zircon (El Kassas, 1974; El Tahir, 1985 and Ahmed, 1991). Pyrite, galena, monazite, muscovite, rutile and cassiterite are also present as accessories (Abu-Deif, 1992). Hydrothermal alterations are common in the form of silicification, kaolinization and argillic alteration as well as sericitization. Jasper is commonly developed as fracture fillings in association with hematitization and limonitization and manganese and iron oxides (El Kassas, 1974; El Tahir, 1985; Mohamed, 1988).

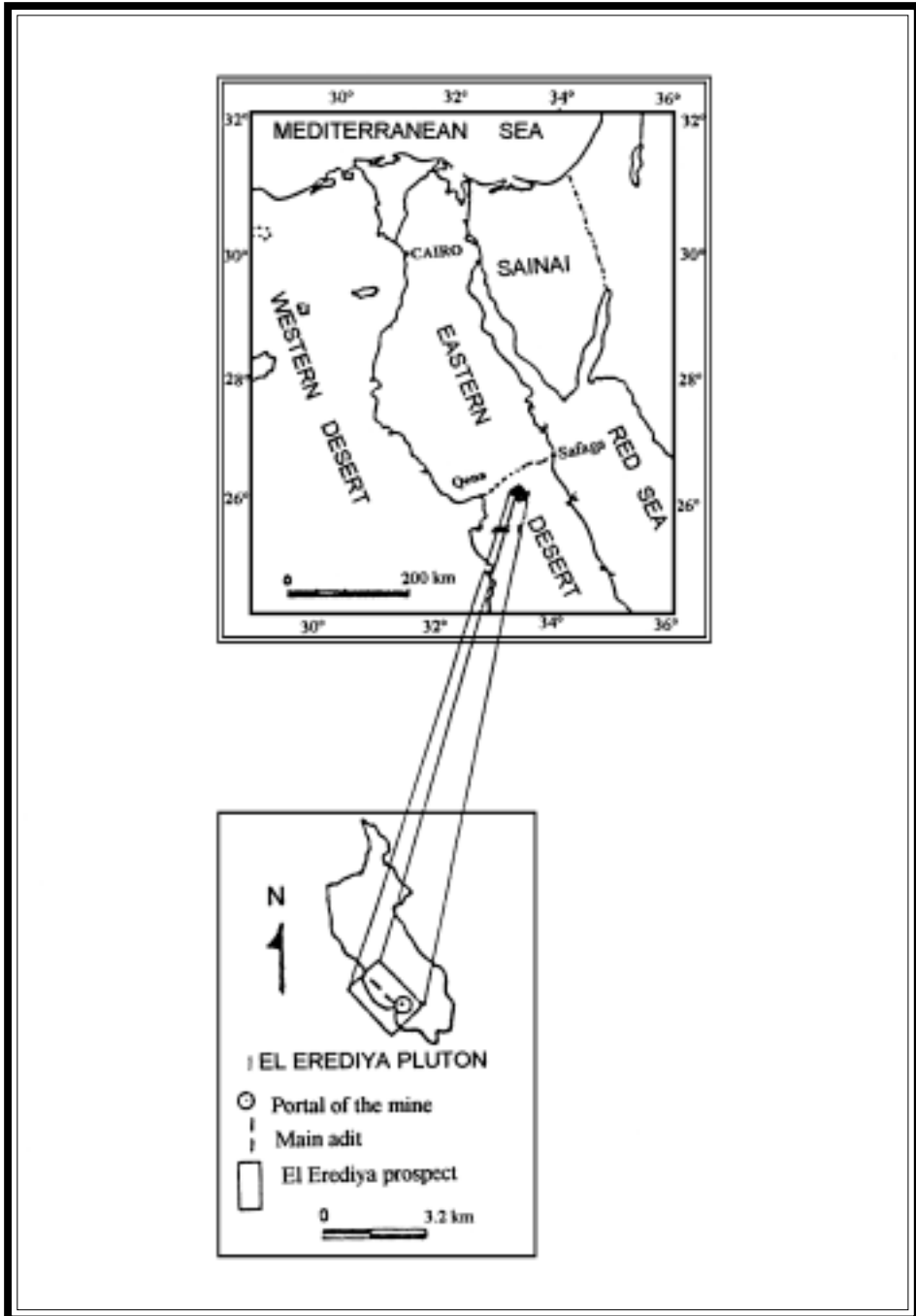


Fig. 1. Location map of G. El Erediya prospect, Central Eastern Desert.

Structurally, the granitic mass of El Erediya is bounded from the northeast and southwest sides by NW trending faults. It is cut by some others trending mainly in NW and N-S directions.

Uranium mineralization, connected mainly to jasperoid veins, trending in N to NE directions, was recorded in the form of small segregation pods and lenses of pitchblende and its secondary alteration products (El Kassas, 1974). El-Erediya uranium occurrence was considered a case of siliceous vein type deposit by Hussein *et al.* (1986).

Exploratory Tunneling Works.

Exploratory tunneling works have commenced in early 1980, at the southern part of El-Erediya mass, Fig. 2. The shear zones were intercepted through the main adit (MA) trending in N50W direction – roughly at wadi level – and perpendicular to the main trend of the shear zones. At the points of the interceptions, drifts (D) were driven following the extensions of some mineralized shear zones. These works showed that the shear zone No. 2 (Sh. Z. 2), explored through DII and DIII, is a uranium-hosting zone, Fig 2. Massive and disseminated pitchblende as well as secondary uranium minerals were detected in this shear zone in three anomalous sections, namely anomaly An IV, An V and An VI (El Tahir, 1985; Hussein *et al.*, 1986). Two of these mineralized sections (An. V and An VI) of about 38 m total extent were selected for the present study, besides a section of about 62 m length in the main adit represents the less altered granite, Fig. 2.

Tunnels Geology and Uranium Mineralization

According to El Tahir (1985) and Hussein *et al.* (1992), the explored rocks in the tunnels are represented mainly by unaltered biotite granite which forms the main bulk of the tunneling works especially at the main adit away from the shear zones. The explored rocks in the drifts include jasperoid veins and veinlets filling fractures of shear zones. Zonally arranged around the jasperoid veins, are the alteration products of the granite. The wall- rock alteration are represented mainly by silicified and mylonitized granite, kaolinized granite and some of limited extension of sericitized granite. Hematitization, limonitization as well as black manganese and iron oxides and some argillaceous materials are also common, Figs. 3 and 4.

The silicified and mylonitized granite appears as hard, compact and red coarse-grained. Mylonitization effects are characterized by crushed appearance of rock, which developed fine streaks, elongations and decreasing granularity of mineral constituents (El Tahir, 1985). Kaolinized granite occurs at the fractured

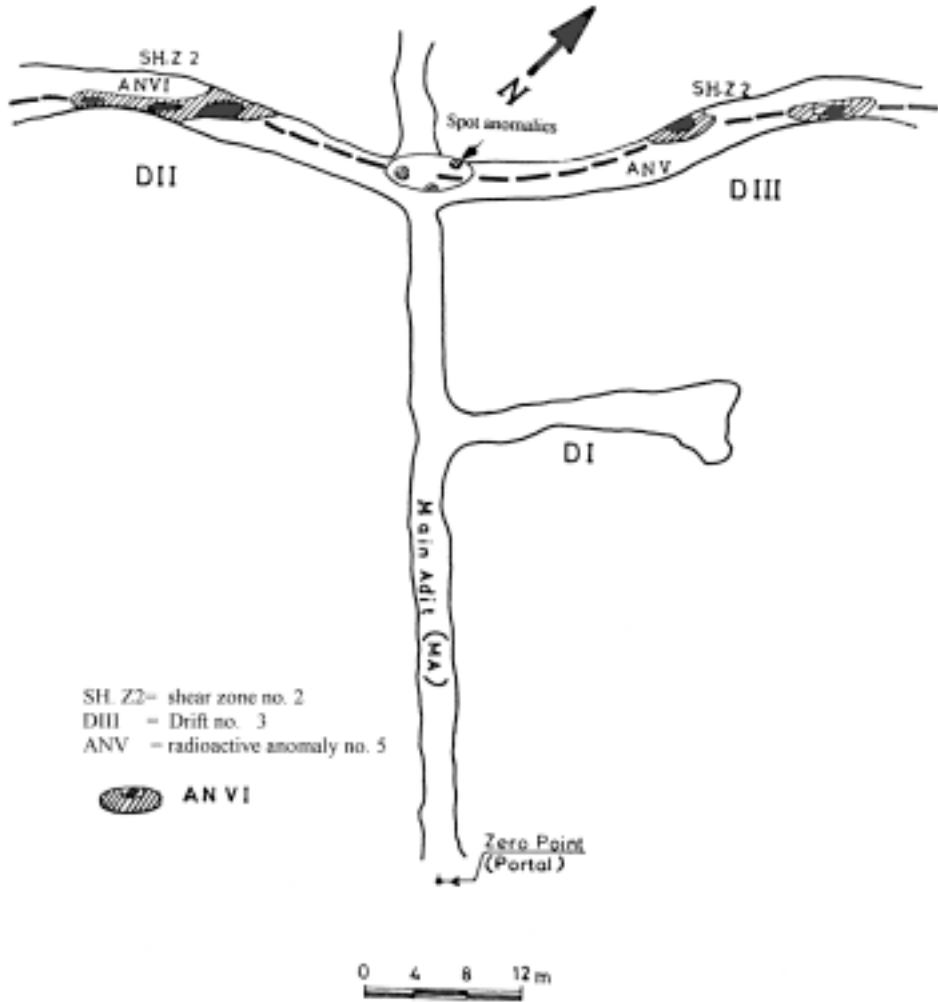


FIG. 2. Sketch map showing the location of An V and An VI in a part of El Erediya mine, Central Eastern Desert, Egypt.

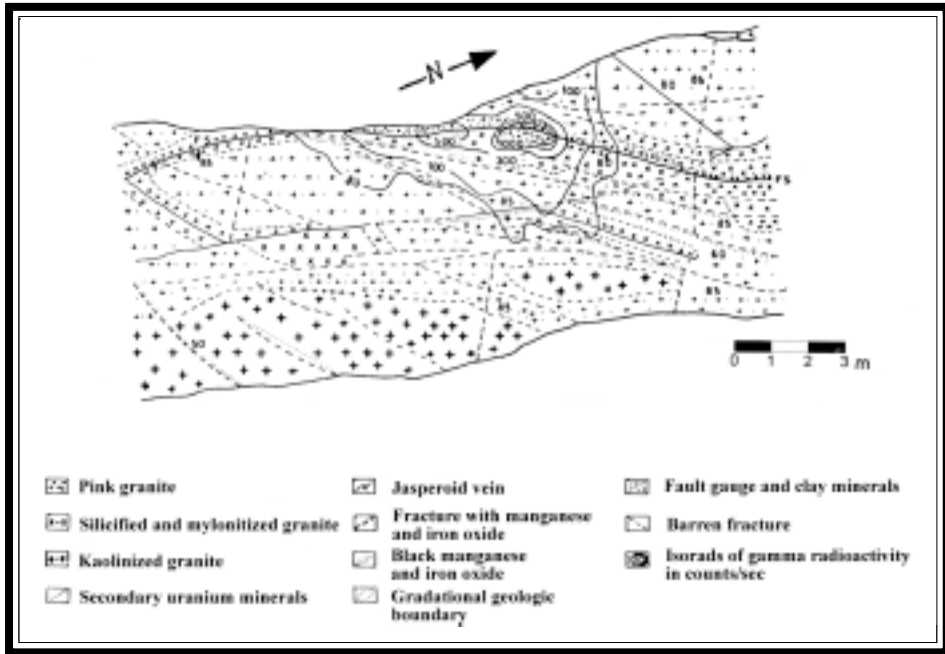


FIG. 3. Geologic and radiometric map of anomaly No. V, drift No. III, El-Erediya mining works (El-Taher, 1985).

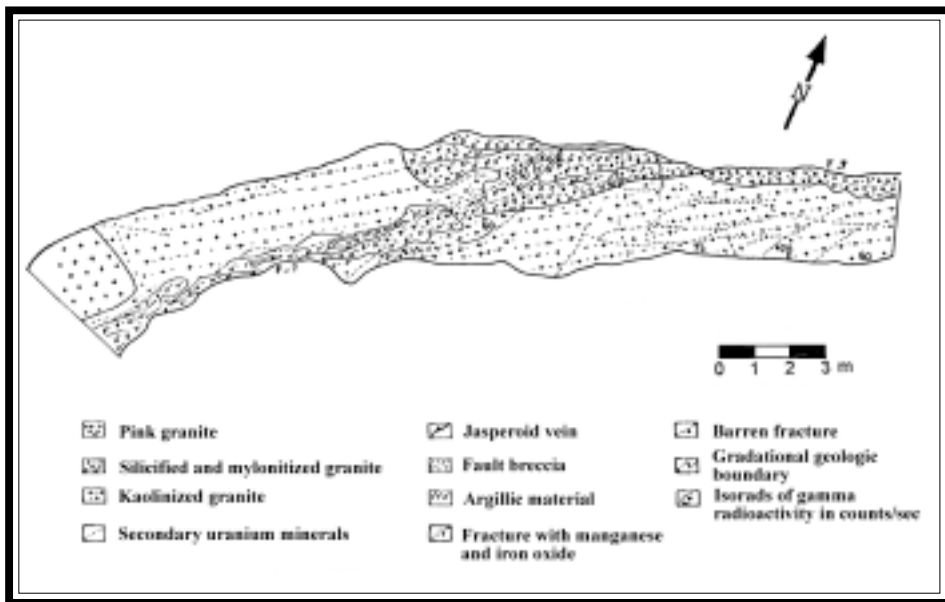


FIG. 4. Geologic and radiometric map of anomaly No. VI, drift No. 11, El-Erediya mining works (El-Taher, 1985).

walls or in contact with the silica filling. In kaolinized granite, feldspars are mostly altered to kaoline; the rock becomes light in colour and more brittle. In some parts the kaolinized granite is sheared with the development of argillic materials as filling along shear planes.

Primary and secondary uranium mineralization was detected in three sections along DII and DIII. They are closely connected to faults and fractures occupied by jasperoid materials which trend mainly in N to ENE directions. The mineralized faults are intensely brecciated. The uranium minerals occur as stains on the hanging wall of the jasperoid veins, as disseminated in the microfractures and as lensoid masses of massive pitchblende enveloped by secondary uranium minerals and protected by two sets of jasperoid silica, Fig. 3. It is worth to mention that, the jasperoid veins are not mineralized, but they act as traps capturing and protecting the U-minerals. The most significant section (An VI) is a thin lens of pitchblende (4 m × 30 cm), enveloped by a thin layer of secondary alteration products rich in secondary U-minerals (El Tahir, 1985). Abu-Deif, (1992) reported a U-Pb age of 130-160 Ma. for El-Erediya pitchblende.

Spectrometric Studies

An extensive gamma-ray spectrometric survey was carried out on two of the mineralized sections in the drifts (An. V and An. VI), besides a considerable part in the main adit. The present spectrometric survey was carried out by Gs-256 spectrometer (with sodium iodide crystal detector 3" diameter by 3" inches long). The measurements are taken through uniform grid pattern of 50 cm. Sixty-seven measurements were taken for correlation in the main adit, 56 measurements in anomaly V location and 152 measurements in anomaly VI location.

The data are represented as maps for anomaly V, Figs. 5, 6, 7, and 8 and anomaly VI, Figs. 12, 13, 14, and 15.

Statistical analysis of the spectrometric data was carried out using a computer program in order to define the distribution pattern of the radioelements in the granite and its alteration products in the mine. Generally, there is a strong relationship between the distribution of different lithological units in the mine and the levels of the spectrometric measurements. Therefore, the spectrometric data were divided into a number of levels, each of which is related to one of the lithologic unit with the same radiometric signature. In this study, statistical computations were applied on the original data without employing any type of transformation. This is in accordance with the work of Sarma and Cock (1980), who recommended the performance of statistical computations on the original data. A variable possesses a coefficient of variability (CV%) is examined [$CV\% = (S/X * 100)$], where S is the standard deviation and X is the arithmetic mean. If

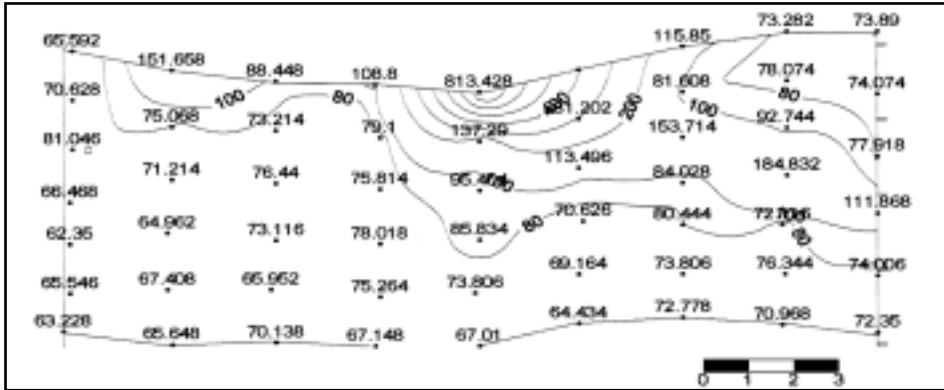


Fig. 5. The total radiometric (in Ur) contour map, DIII, AN, V, El-Erediya mine, Central Eastern Desert.

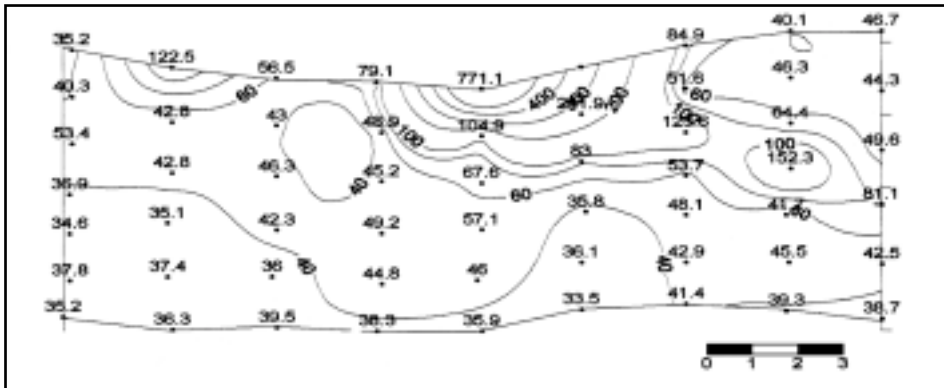


Fig. 6. The equivalent uranium (in ppm) contour map, DIII, AN, V, El-Erediya mine, Central Eastern Desert.

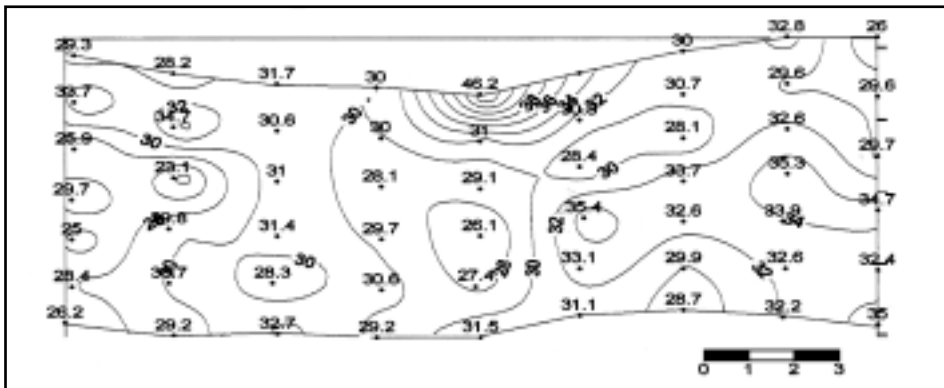


Fig. 7. The equivalent thorium (in ppm) contour map, DIII, AN, V, El-Erediya mine, Central Eastern Desert.

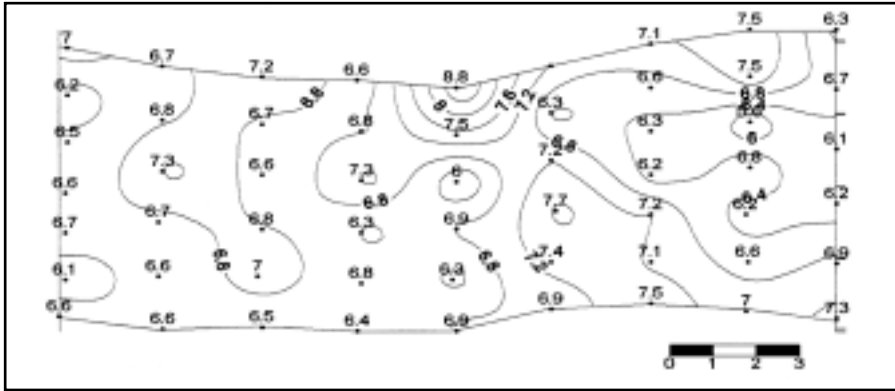


FIG. 8. The potassium percentage contour map, DIII, AN, V, El-Erediya mine, Central Eastern Desert.

(CV%) for a certain unit is less than 100%, the radioelement variability in the unit tends to exhibit normal distribution. The computed values for (S) and (X) of the total count activity (in Ur), the absolute potassium (K in %), equivalent uranium (eU in ppm), and equivalent thorium (eTh in ppm) concentrations as well as their ratios in the tunnels are shown in Tables 1-3.

TABLE 1. Statistical treatments of the raw spectrometric data of the main adit, the two anomalous zones and all data.

| Body | No. of values | Statistical elements | T.C. (Ur) | K (%) | eU (ppm) | eTh (ppm) | eU/eTh | eU/K% *10 ⁻⁴ | eTH/K% *10 ⁻⁴ | |
|----------------|---------------|----------------------|-----------|-------|----------|-----------|--------|-------------------------|--------------------------|--|
| Main Adit | 67 | Min | 42.7 | 5.2 | 14.8 | 21.9 | 0.7 | 2.8 | 4.2 | |
| | | Max | 76.7 | 8.4 | 50.8 | 33.4 | 1.5 | 6.0 | 4.0 | |
| | | X | 52 | 6.4 | 24.4 | 26.7 | 0.9 | 3.8 | 4.2 | |
| | | S | 6 | 0.5 | 6.8 | 2.7 | 2.5 | 12.5 | 5.4 | |
| | | CV% | 11.5 | 7.8 | 27.9 | 10.1 | | | | |
| Anomaly Zone V | 56 | Min. | 62.4 | 5.6 | 33.5 | 23.1 | 1.5 | 6.0 | 4.1 | |
| | | Max. | 813.4 | 8.8 | 771.1 | 46.2 | 16.7 | 87.6 | 5.3 | |
| | | X | 99.4 | 6.8 | 69.0 | 30.7 | 2.2 | 10.2 | 4.5 | |
| | | S | 103.6 | 0.5 | 102.1 | 3.4 | 29.9 | 194.5 | 6.5 | |
| | | CV% | 104.2 | 7.4 | 148.0 | 11.1 | | | | |
| | | Min. | 53.4 | 3.8 | 23.2 | 22.1 | 1.0 | 6.1 | 5.8 | |
| | | Max. | 480.8 | 7.8 | 450.7 | 56.8 | 7.9 | 57.8 | 7.3 | |

TABLE 1. Contd.

| Body | No. of values | Statistical elements | T.C. (Ur) | K (%) | eU (ppm) | eTh (ppm) | eU/eTh | eU/K% *10 ⁻⁴ | eTh/K% *10 ⁻⁴ |
|-----------------|---------------|----------------------|-----------|-------|----------|-----------|--------|-------------------------|--------------------------|
| Anomaly Zone VI | 152 | X | 105.2 | 6.6 | 75.5 | 30.1 | 2.5 | 11.5 | 4.6 |
| | | S | 76.4 | 0.7 | 77.6 | 4.2 | 18.6 | 111.4 | 6.0 |
| | | CV% | 72.6 | 10.6 | 102.8 | 14.0 | | | |
| All Data | 275 | Min. | 42.7 | 3.8 | 14.8 | 21.9 | 0.7 | 3.9 | 5.8 |
| | | Max. | 482.4 | 8.8 | 771.1 | 856.5 | 0.9 | 87.6 | 10.4 |
| | | X | 87.1 | 6.6 | 61.7 | 29.4 | 2.1 | 9.4 | 5.9 |
| | | S | 62.3 | 0.6 | 76.7 | 4.0 | 19.2 | 119.3 | 25.0 |
| | | CV% | 71.5 | 9.1 | 124.3 | 13.6 | | | |

X = arithmetic mean, S = standard deviation, CV = coefficient of variation, Min = minimum value & Max = maximum value

TABLE 2. Statistical treatments of anomaly V in drift III.

| Anomaly Zone V | Statistical elements | T.C. (Ur) | K (%) | eU (ppm) | eTh (ppm) | eU/eTh | eU/K% | eTh/K% |
|--|----------------------|-----------|-------|----------|-----------|--------|-------|--------|
| Unit V-1 Pink granite | Min | 65.6 | 6.2 | 35.2 | 28.2 | 1.2 | 5.7 | 4.5 |
| | Max | 813.4 | 8.8 | 771.1 | 46.2 | 16.7 | 87.6 | 5.3 |
| | X | 157.9 | 6.8 | 126.5 | 32.5 | 3.9 | 18.5 | 4.8 |
| | S | 197.0 | 0.7 | 194.0 | 4.4 | 43.8 | 283.3 | 6.5 |
| | CV% | 124.7 | 102.9 | 153.4 | 13.5 | | | |
| Unit V-2 Silicified mylonitized granite | Min | 65.0 | 6.1 | 35.1 | 26.1 | 1.3 | 5.8 | 4.3 |
| | Max | 184.8 | 7.5 | 152.3 | 35.3 | 4.3 | 20.3 | 4.7 |
| | X | 87.2 | 6.7 | 57.0 | 30.3 | 1.9 | 8.5 | 4.5 |
| | S | 34.6 | 0.4 | 34.5 | 2.3 | 14.9 | 78.5 | 5.3 |
| | CV% | 39.7 | 6.0 | 60.5 | 7.6 | | | |
| Unit V-3 Kaolinitized granite | Min | 62.4 | 5.6 | 33.5 | 23.1 | 1.5 | 6.0 | 4.1 |
| | Max | 115.9 | 7.7 | 84.9 | 35.4 | 2.4 | 11.0 | 4.6 |
| | X | 75.5 | 6.8 | 45.4 | 29.9 | 1.5 | 6.7 | 4.4 |
| | S | 11.3 | 0.5 | 11.6 | 3.1 | 3.8 | 23.6 | 6.3 |
| | CV% | 15.0 | 7.4 | 25.6 | 10.4 | | | |

TABLE 3. Statistical treatments of anomaly No. VI .

| Anomaly Zone VI | Statistical elements | T.C. (Ur) | K (%) | eU (ppm) | eTh (ppm) | eU/eTh | eU/K% | eTh/K% |
|---|----------------------|-----------|-------|----------|-----------|--------|-------|--------|
| Unit VI-1 Silicified granite | Min | 61.4 | 5.8 | 32.2 | 24.2 | 1.3 | 5.6 | 4.2 |
| | Max | 122.0 | 7.1 | 94.0 | 30.7 | 3.1 | 13.2 | 4.3 |
| | X | 89.5 | 6.3 | 61.6 | 27.6 | 2.2 | 9.8 | 4.4 |
| | S | 22.8 | 0.5 | 23.2 | 2.8 | 8.4 | 44.4 | 5.6 |
| | CV% | 25.5 | 7.9 | 37.7 | 10.1 | | | |
| Unit VI-2 Kaolinized granite having more fractures | Min | 54.4 | 5.3 | 23.2 | 24.5 | 0.9 | 4.4 | 4.6 |
| | Max | 421.7 | 7.8 | 39.7 | 56.8 | 7.0 | 5.1 | 7.3 |
| | X | 86.5 | 6.9 | 54.9 | 32.4 | 1.7 | 7.9 | 4.7 |
| | S | 63.8 | 0.5 | 65.0 | 5.0 | 13.0 | 131.5 | 10.0 |
| | CV% | 73.8 | 7.2 | 118.4 | 15.4 | | | |
| Unit VI-3 Kaolinized granite having less fractures | Min | 58.2 | 6.0 | 28.2 | 22.1 | 1.3 | 4.7 | 3.7 |
| | Max | 94.4 | 7.7 | 66.0 | 32.4 | 2.0 | 8.6 | 4.2 |
| | X | 68.8 | 6.9 | 39.1 | 28.6 | 1.4 | 5.7 | 4.1 |
| | S | 7.9 | 0.5 | 8.4 | 2.5 | 3.4 | 18.3 | 5.0 |
| | CV% | 11.5 | 7.2 | 21.5 | 8.7 | | | |
| Unit VI-4 Silicified granite | Min | 55.2 | 5.4 | 26.0 | 25.5 | 1.0 | 4.8 | 4.7 |
| | Max | 480.8 | 6.7 | 450.7 | 33.1 | 13.6 | 67.3 | 4.9 |
| | X | 152.2 | 6.0 | 124.5 | 28.7 | 4.3 | 20.6 | 4.8 |
| | S | 130.4 | 0.4 | 130.2 | 2.3 | 57.3 | 340.8 | 5.8 |
| | CV% | 85.7 | 6.7 | 104.6 | 8.0 | | | |
| Unit VI-5 Silicified granite associated with jasper mineralization | Min | 68.0 | 3.8 | 37.1 | 23.1 | 1.6 | 9.8 | 6.1 |
| | Max | 369.2 | 7.1 | 344.3 | 37.0 | 9.3 | 48.5 | 5.2 |
| | X | 163.3 | 6.0 | 135.6 | 29.0 | 4.7 | 22.8 | 4.3 |
| | S | 80.1 | 0.8 | 81.5 | 3.6 | 22.8 | 99.1 | 4.5 |
| | CV% | 49 | 13.3 | 60.1 | 12.4 | | | |
| Unit VI-6 Pink granite | Min | 53.4 | 6.2 | 26.1 | 25.8 | 1.0 | 4.2 | 4.2 |
| | Max | 104.3 | 7.2 | 72.5 | 31.4 | 2.3 | 10.1 | 4.4 |
| | X | 72.4 | 6.8 | 42.7 | 28.6 | 1.5 | 6.3 | 4.2 |
| | S | 20.4 | 0.4 | 19.7 | 2.2 | 8.8 | 52.3 | 5.5 |
| | CV% | 28.2 | 5.9 | 46.1 | 7.7 | | | |

In addition, the probability plot is used to evaluate the normality of the distribution of the total count radiometric data, that is, whether and to what extent the distribution of this variable follows the normal distribution. The observed variables were plotted on a standard normal probability plot (Geigy, 1962).

The normal probability plots for anomaly V, Fig. 9, and anomaly VI, Fig. 16 show that the distribution of the total count radiometric data for both anomalies are not normal, and each of them include more than one population. As a result, the anomaly V is divided into three different interpreted radiometric lithologic (IRL) units, each of which possesses different radiometric level and corresponds to three petrographical rock types, Fig. 10. The resultant outlines of these units are shown in, Fig. 11. Meanwhile, the anomaly VI, Fig. 17, contains six IRL units, Fig. 18.

Uranium Migration

Uranium and thorium are usually accompanied together during geologic unit formation due to the similarity in their ionic radii. During the evolution of the crust, U^{+4} is easy to oxidize and migrate, whereas Th is stable in the oxidation zone. So, we can consider Th as a reference to study the original U-state.

The U/Th ratio is a very important geochemical index for U migration, it is an approximate constant in the same type of rock or geologic unit in a relatively closed environment. The uranium migration (out or in) has the same probability within geologic units in relatively closed geologic environment. The half-life periods of uranium and thorium are very long, so the present U/Th ratio can be considered as original U/Th ratio (in closed environment).

According to the NMA Scientific Internal Report (1999), the uranium migration value (U_m) for a certain rock unit can be obtained by subtracting the original uranium content U_o (or paleo-uranium background) from the present uranium content U_p (or the actual measured one), where $U_m = U_p - U_o$. The original uranium content (U_o) can be theoretically calculated according to the equation:

$$U_o = e_{Th} * (\text{regional } eU/eTh) \quad (1)$$

where e_{Th} is the average thorium content in a certain geologic unit (ppm); (regional eU/eTh) means the average regional eU/eTh ratio in different geologic units.

Then, the U-migration rate (U-mr %) can be calculated by the following equation:

$$U\text{-mr \%} = U_m * 100/U_p \quad (2)$$

The rate of uranium migration is also a good indicator for determining type and degree of migration. If it is positive; the migration is in, and if it is negative; the migration is out.

If $(U_m) > 2$ indicates that uranium has been lost from the geologic body during later evolution. $(U_m) < -2$ indicates that a considerable amount of uranium has migrated into the rock unit. $-2 < (U_m) < 2$ points to the high probability that migration is equivalent in and out of the rock unit.

Discussion and Interpretation

Qualitative and Quantitative Interpretation of Spectrometric Data

The geologic maps of anomalies V and VI are presented in Figs. 3 & 4 and their spectrometric maps are presented in Figs. 5-8 and 12-15 respectively. The main results drawn from analysis of raw spectrometric data of the two chosen anomalous zones and the main adit are given in Table 1.

The Main Adit

The total counts in the main adit, that mainly represent the unaltered pink granite, range from 42.7 to 76.7 Ur, with an average of about 52 Ur. The contents of the three radioelements (U, Th and K) and their ratios are given in Table 1. The results show that this granite is U-rich granite. It has uranium content of about 24.4 ppm. It also has some high Th content relative to the two anomalous zones. As a result, this granite has the lowest eU/eTh ratio (0.9) and the highest eTh/K ratio (4.2) relative to the two mineralized sections, Table 1.

Anomaly V

This anomalous zone has a wide range of radioactivity ranging from 37.9 Ur to 813.4 Ur with an average of about 99.4 Ur, Table 1.

The normal probability plot for this anomaly, Fig. 9, shows that the distribution of the total count radiometric data is not normal. It could be divided into three populations (V1, V2 and V3); each has normal distribution, Fig. 10, corresponding to three IRL units. Each of these units (V1, V2 and V3) has its own geologic and radiometric features. The lithoradiometric unit map of this anomaly, Fig. 11, is conformable with the geologic map of this mineralized section, Fig. 3.

The first IRL unit (V1) represents the pink granite, V2 represents the mylonitized granite with jasperoid veins and V3 represents the kaolinized granite. The location of the NE-SW and NW-SE fractures can be detected easily.

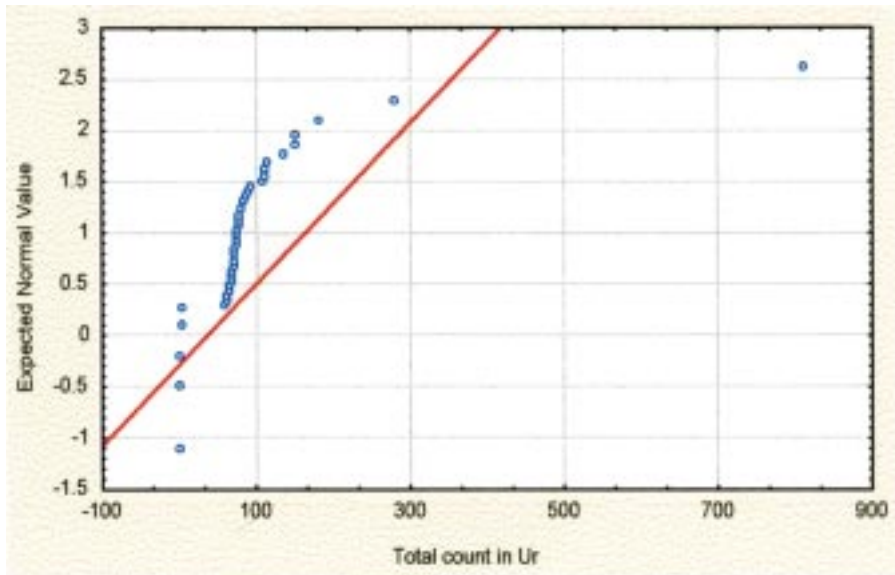


FIG. 9. Normal probability plot of total count radiometric data, for AN, V Drift III, El-Erediya mine, Central Eastern Desert, Egypt.

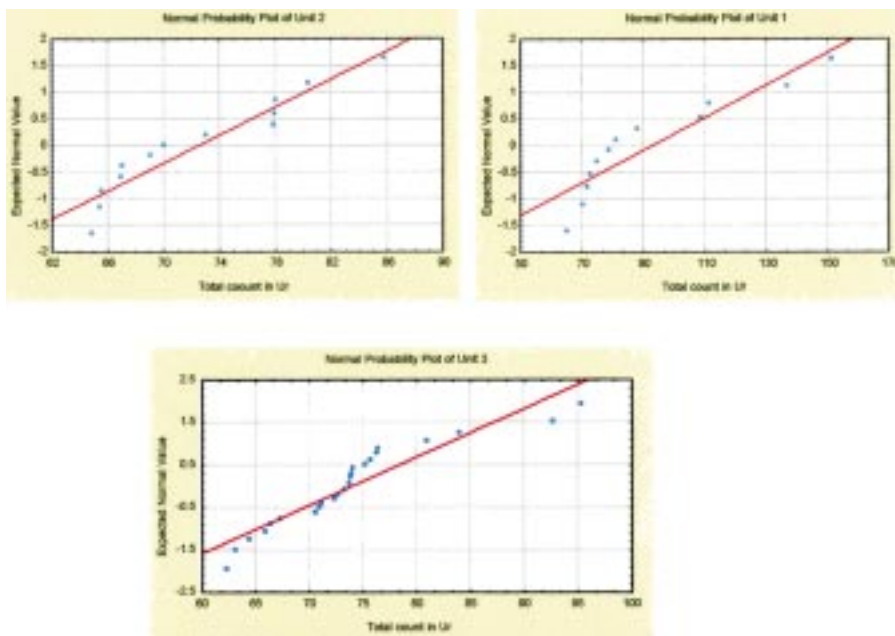


FIG. 10. Normal probability plots of total count radiometric data, for units 1, 2 and 3, El-Erediya Mine, An V, Drift No. III, Central Eastern Desert, Egypt.

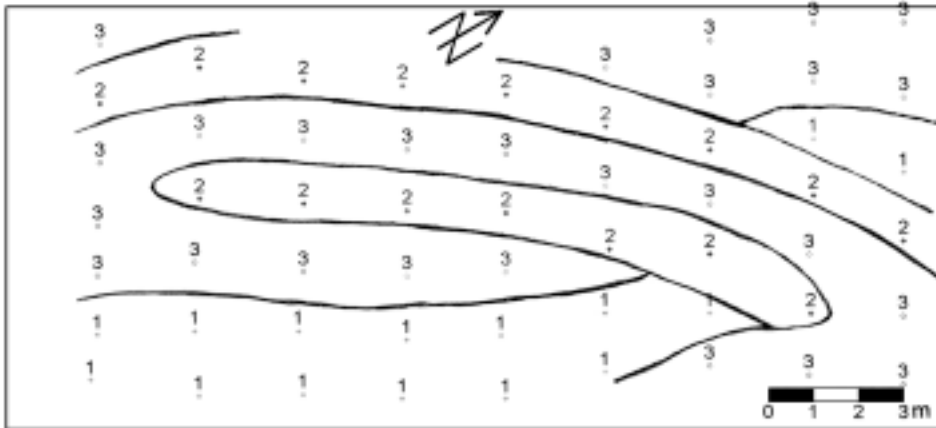


FIG. 11. Lithoradiometric unit map of An V, Drift III, El-Erediya Mine, Central Eastern Desert, Egypt.

Table 2 shows the main results of the statistical treatment of An V. It is clear from this table that the second unit (V2), which includes the silicified and jasperoid veins, has relatively the highest content of uranium among the other units. As a result, it has also the highest eU/eTh and eU/K ratios.

Anomaly VI

The total counts of the raw data of this anomalous zone show a wide variation ranging from 53.4 Ur to 480.8 Ur, with an average of about 105.2 Ur. The potassium, equivalent uranium and equivalent thorium contents of this anomalous zone range from 3.8 to 7.8%, 23.2 to 450.7 ppm and 22.1 to 56.8 ppm respectively. The average abundance of these radioactive elements in this zone is 6.6 %, 75.5 ppm and 30.1 ppm for K, U and Th respectively Table 1.

The NE trend of fracturing is shown clearly on the spectrometric maps, Figs. 12-15, in addition to the perpendicular NW trend that dissects the NE trend. According to the spectrometric maps, Figs. 12-15, the geologic map of this anomalous zone, Fig. 4 and the probability plots, Figs. 16 and 17, this anomalous zone can be divided into six lithoradiometric units (VI-1 to VI-6), Fig. 18 which differ in their radioelement contents. These IRL units are conformable with the geologic units included in the geologic map, Fig. 4. Each of these six units has its own characteristic features in both lithology and radiometry. However, these units correspond only to three main lithologic units (silicified, kaolinized and pink granites). Units VI-1, VI-4 and VI-5 are related to the silicified granite; whereas units VI-2 and VI-3 are related to the kaolinized granite. Unit VI-6 represents the less altered pink granite. Although there is no significant difference in the lithology between the three units of the silicified granites or the two units

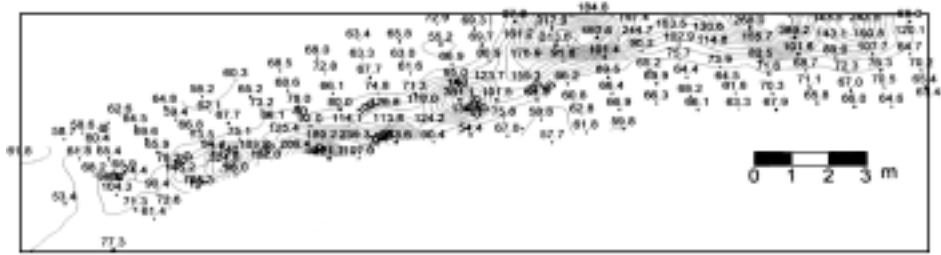


FIG. 12. The total radiometric (in ur) contour map, DII, Anomaly VI, El-Erediya mine, Central Eastern Desert, Egypt.

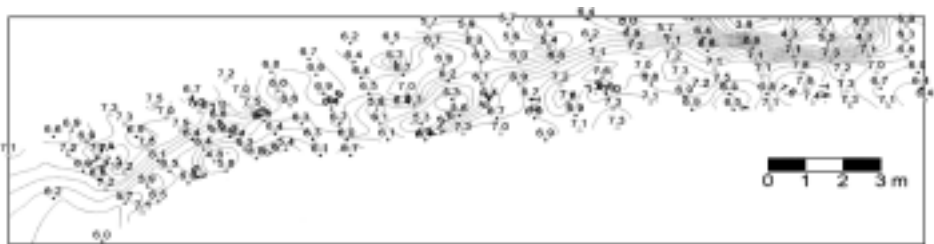


FIG. 13. The potassium percentage contour map, DII, Anomaly VI, El-Erediya mine, Central Eastern Desert, Egypt.

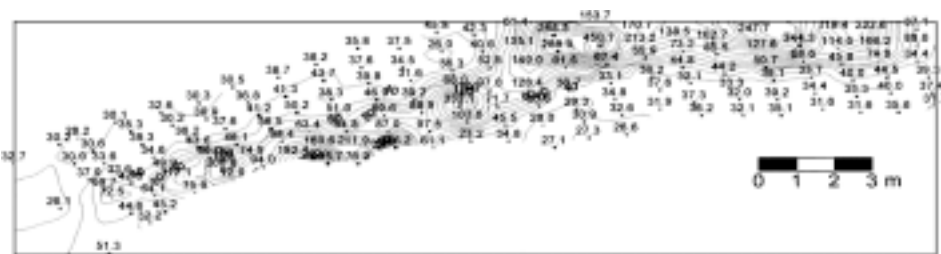


FIG. 14. The equivalent uranium (in ppm) contour map, DII, Anomaly VI, El-Erediya mine, Central Eastern Desert, Egypt.

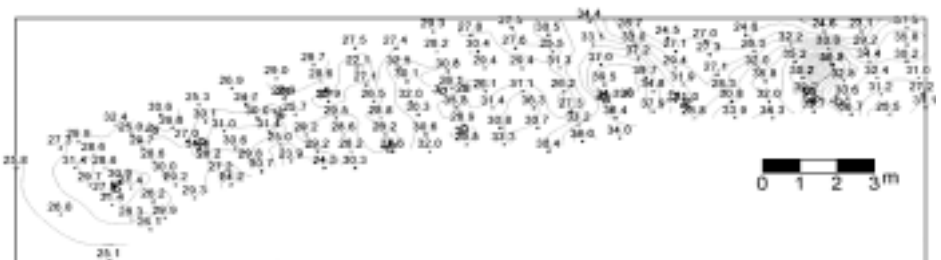


FIG. 15. The equivalent thorium (in ppm) contour map, DII, Anomaly VI, El-Erediya mine, Central Eastern Desert, Egypt.

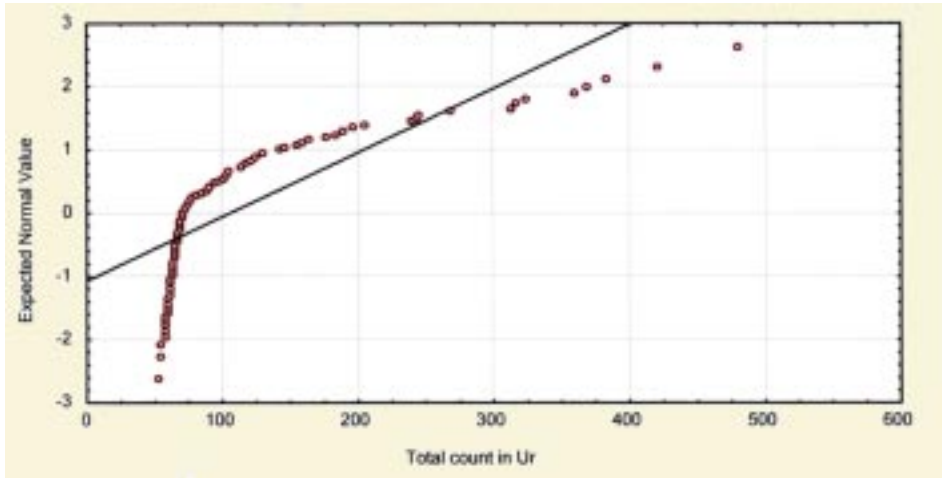


FIG. 16. Normal probability plots of total count radiometric data for AN, Drift II, El-Ereidiya mine, Central Eastern Desert.

of the kaolinized granites, it could be differentiated between these units by using the probability plots. This is due to some small geologic and structural differences such as the intensity of the alteration and fracturing, Fig. 4 & Table 3. The main results of the statistical treatment of An VI data are given in Table 3.

It is clear from Table 3 that the two units 4 and 5 have the highest radioelement contents, unit 4 is related to the silicified and mylonitized granite, whereas unit 5 is related to fault breccia with jasperoid veins. The kaolinized granites, represented by unit-2 has a relatively moderate amount of radioelement contents, while the pink granite (unit 6) and kaolinized granite (unit-3) have least amounts of the radioelement contents, compared by the previous units. The distribution of the uranium in the six units is nearly similar to that of the total count, while the Th and K contents do differ, as they increase in the northern part of this anomalous zone especially in the kaolinized granite and along minor faults.

Uranium Migration

From the statistical treatment of the spectrometric data of the two anomalous zones and the main adit, the regional eU/eTh is 2.1, Table 1. After the calculation of U_0 (original uranium content, according the eq. No. 1) in the main adit and the two drifts and in their classified units, the main results of the migration are shown in Table 4. It shows that the pink granite (the main rock of the main adit, units V-1 and VI-6) have a high outward uranium migration. This outside migration is shown also in unit 3 of anomaly V and units 2 and 3 of anomaly VI, which are related to the kaolinized granite. Close examination of this table shows that the inward migration is indicated in the silicified granite units of the

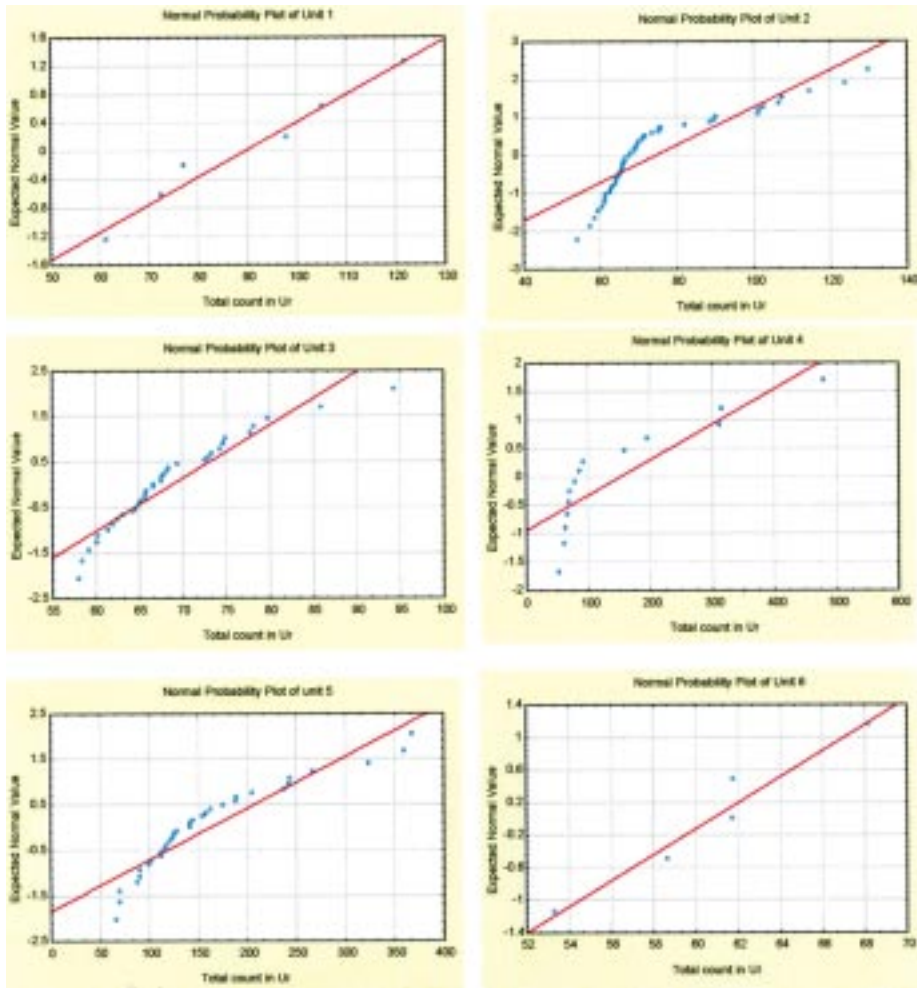


FIG. 17. Normal probability plot of total count radiometric data, for units from 1 to 6, El-Erediya Mine, An VI, Drift III, El-Erediya Mine, Central Eastern Desert.

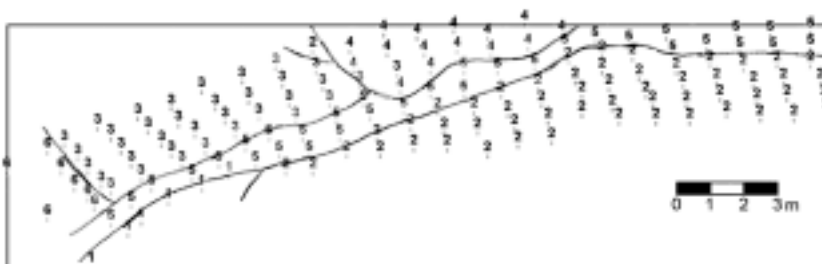


FIG. 18. Lithoradiometric unit map of An VI, Drift III, El-Erediya Mine, Central Eastern Desert, Egypt.

two anomalous zones (anomaly V and anomaly VI). The percent inward migration increases with the increasing of silicification and fracturing, beside the relative increase in the jasperoid products and mylonization of the granite.

TABLE 4. Migration direction of uranium in the different litho-spectrometric units, El-Erediya exploratory tunnels, Central Eastern Desert, Egypt.

| Bodies | Present uranium Up | Original uranium Uo | Migrated uranium Um | U-migrated rate % U-mr | Remarks |
|--|------------------------------|-------------------------------|-------------------------------|----------------------------------|---------------------|
| Main Adit Pink granite | 24.4 | 56.7 | -32.3 | -132.4 | Outward migration ↑ |
| An V | 69.0 | 64.5 | 4.5 | 6.5 | Inward migration ↓ |
| Unit V-1 Pink granite | 57.0 | 63.6 | -6.6 | -11.7 | Outward migration ↑ |
| Unit V-2 Silicified mylonitized granite | 126.5 | 68.3 | 58.2 | 46.0 | Inward migration ↓ |
| Unit V-3 Kaolinized granite | 45.4 | 62.8 | -17.4 | -38.3 | Outward migration ↑ |
| An VI | 75.5 | 63.2 | 12.3 | 16.3 | Inward migration ↓ |
| Unit VI-1 Silicified granite | 61.6 | 58.0 | 3.6 | 5.8 | Inward migration ↓ |
| Unit VI-2 Kaolinized granite having more fracture | 54.9 | 68.0 | -13.4 | -23.9 | Outward migration ↑ |
| Unit VI-3 Kaolinized granite having less fractures | 39.1 | 60.1 | -21 | -53.6 | Outward migration ↑ |
| Unit VI-4 Silicified granite associate with jasper | 124.5 | 60.3 | 64.2 | 51.6 | Inward migration ↓ |
| Unit VI-5 Silicified granite | 135.6 | 60.9 | 74.7 | 55.1 | Inward migration ↓ |
| Unit VI-6 Pink granite | 42.7 | 60.1 | -17.4 | -40.7 | Outward migration ↑ |

$$U_o = eTh \times (\text{regional } eU/eTh). \quad U_m = U_p - U_o. \quad U\text{-mr } \% = U_m \times 100 / U_p$$

Conclusions

The pink granite of El Erediya tunnels is relatively Th rich, as Th/K ratio ≥ 2 while the eU/eTh < 1 , which means that this granite is relatively depleted in uranium. The two anomalous zones show some enrichment of uranium. The pink granite and the kaolinized granite show very high probability of uranium migration. In other words, the outward uranium migration shows the highest rate of migration. The inward uranium migration into the units is indicated in the silicified granite of the two anomalous zone (An V and An VI). The percent of inward migration increases with the increase of silicification and fracturing, beside the relative increase in the jasperoid products. The preceding facts indicate that the source of U-mineralization in El Erediya post-tectonic granite is probably the granite itself. The enrichment of uranium in the silicified granite is probably due to mobilization of uranium from granite, which show some degree of outward migration; especially from the kaolinized part into its present localization within the shear and fracture zones.

Acknowledgements

The authors would like to express their gratitude and acknowledgements to Prof. Dr. Kadry M. Foad, Nuclear Materials Authority for revising the manuscript of this paper and for his valuable discussions and comments.

References

- Abu-Deif, A.** (1992) The relation between the uranium mineralization and tectonics in some Pan-African granites, west of Safaga, Eastern desert, Egypt. *Ph. D. Thesis, Assiut Univ.*, Egypt, 218 p.
- Ahmed, N. A.** (1991) Comparative studies of the accessory heavy minerals in some radioactive rocks of G. El Misskat and G. El Erediya, Eastern Desert, Egypt and their alluvial deposits, *M. Sc. Thesis*, Cairo Univ., Egypt, 244P.
- Darnley, and Ford, K.L.** (1989) A Regional Airborne Gamma-ray Surveys Review; in Proceedings of Exploration, 87: Third Decennial International Conference on Geophysical and Geochemical Exploration for Minerals and Groundwater, edited by G.D. Garland, Ontario, *Geol. Surv. of Canada*, Special. **3**, 960 p.
- El Kassas I.A.** (1974) Radioactivity and Geology of Wadi Atalla Area, Eastern Desert of Egypt., A.R.E. *Ph.D. Thesis, Faculty of Science, Ein Shams University*, Cairo, 502.P.
- El-Tahir,** (1985) Radioactivity and mineralization of granitic rocks of El Erediya occurrence and comparison to El Missikat-Rei El-Garra occurrence, Eastern Desert, Egypt. *Ph.D. Thesis, Al Azhar Univ.*, Egypt
- Fullagar, P.D.** (1980) Pan African age granites of northeastern Africa: new or reworked sialic materials. In: **M. J. Salem** and **M. T. Busrewil** "eds." *The geology of Libya*, Acad. Press, Ill., pp. 1051-1053.
- Geigy, J.R.** (1962) Documenta Geigy Scientific Tables. 6th ed., edited by Konrad
- Greenberg, J.K.** (1981) Characteristic and origin of Egyptian younger granites, *Geol. Soc. Am.*, **92**: 749-840.

- Hussein, H.A., Hassan, M. A., El Tahir, M. A. and Abu-Deif, A.** (1986) Uranium bearing siliceous veins in younger granites, Eastern Desert, Egypt, Report of the working group on uranium geology, *IAEA*, Vienna, TECDOC. 361, pp. 143-157.
- Hussein, H.A., Eltair, M.A. and Abu-Deif, A.** (1992) Uranium mineralization through exploratory mining works, South Qena-Safaga midway, Eastern Desert, Egypt, *3rd. Mining, Petroleum and Metallurgy Conference, Cairo Univ.*, **1**: 92-105.
- Mohammed, N.A.** (1988) Mineralogical and petrographical characteristics of some alteration products related to U-mineralization in El Missikat-El Erediya areas, Eastern Desert, Egypt. *M. Sc. Thesis*, Cairo Univ., 110 p.
- NMA Internal Scientific Report** (1999) Study of Abu Zinima area, South Sinai, Egypt.
- Ong, Y.H. and Mior Shallehuddin, B.M.J.** (1988) Promising uranium the Central Belt Area, Peninsular Malaysia, in uranium deposits in Asia and the Pacific: Geology and exploration, Vienna, Austria, pp. 97-107, *Prospects in IAEA-Tc-543/7*.
- Pitkin, J.A. and Duval, J.S.** (1980) Design parameters for aerial gamma-ray surveys. *Geophysics*, **45**(9): 1427-1439.
- Sarma, D.D. and Koch, G.S.** (1980) A statistical analysis of exploration geochemical data for uranium: *Mathematical Geology*, **12**(2): 99-114.
- Stern, R.J. and Hedge, C.E.** (1985) Geochronologic and isotopic constraints on late Precambrian crustal evolution in the Central Eastern Desert of Egypt. *Am. J. Sci.*, pp. 168-172.

توزيع العناصر المشعة وعلاقته بهجرة اليورانيوم - أنفاق العرضية الاستكشافية ، وسط الصحراء الشرقية - مصر

علي أبو ضيف أحمد ، حلمى صلاح عثمان أبو النجا

و حمدى إسماعيل السيد حسانين

هيئة المواد النووية - ص ب ٥٣٠ المعادى - القاهرة - مصر

المستخلص . في عام ١٩٧٠ م اكتشفت تمعدنات اليورانيوم مصاحبة لعروق الجاسبر التي توجد فى نطاقات القص و الشقوق، وذلك فى كتلة الجرانيت بعد التكتونى المكونة لجبل العرضية فى وسط الصحراء الشرقية بمصر. وقد حفرت الأنفاق الاستكشافية بمستوى الوادى متتبعه نطاقات القص حتى يمكن تحديد امتدادات الأجزاء المتمعدنة وتقييم إمكانياتها. وقد كشفت أعمال الأنفاق عن وجود البتشلند (كتلى ومبعثر) بالإضافة إلى مصاحباته الثانوية فى نطاقات القص المستكشفة. وقد وجد أن الجرانيت على طول نطاقات القص غالبا ما يكون متحللا، ومن ظواهر التحلل الأساسية السلكتة والطحن والتحلل الطيني وإلى درجة أقل تكون السريسييت. تم مسح قطاعين متمعدنين بالإضافة إلى الجرانيت غير المتحلل مسحا طيفيا مكثفا و عولجت البيانات إحصائيا لكي نقيم احتمالية وجود اليورانيوم ونحدد اتجاهات هجرته. وقد أوضحت الدراسة وجود علاقة قوية بين توزيع العناصر المشعة ونوع الصخور. وقد بينت الدراسة أيضا حدوث هجرة لليورانيوم إلى داخل معظم الوحدات الصخرية وخاصة الجرانيت السليكاتى فى حين تكون الهجرة إلى الخارج فى حالة الجرانيت الوردى. ذو التحلل الطيني .